J. Fluid Mech. (1990), *pp.* 213, 251–265
Printed in Great Britain

The shape and stability of liquid menisci at solid edges

By DIETER LANGBEIN
Battelle-Institut e.V., Am Römerhof 56, Postfach 90, D-6000 Frankfurt am Main 90, West Germany

(Received 17 September 1988 and in revised form 30 August 1989)

The shape and stability of liquid menisci attached to a solid edge with dihedral angle 2α is investigated. It is shown that in addition to the family of cylindrical menisci a family of azimuthally modified unduloids exists. A double Fourier series of the latter with respect to their axis (parallel to the extension of the edge) and with respect to the azimuth is derived. The dispersion relation between the axial wavenumber q, the azimuthal wavenumber s and the waviness parameter d is calculated. When the condition of constant contact angle γ along the contact lines with the solid is applied, a one-dimensional family of modified unduloids fitting to the edge is obtained. Their axial wavenumber q becomes independent of the waviness d at the bifurcation with the family of cylindrical menisci, such that this bifurcation limits the stability. The respective stability criteria are derived and evaluated. For $\alpha+\gamma > \frac{1}{2}\pi$ the cylindrical menisci are convex. They reveal a maximum stable length, which quadratically tends to infinity when $\alpha+\gamma = \frac{1}{2}\pi$ is approached. The smallest stable extension arises for the free cylindrical column (the Rayleigh jet), which is covered by the present investigations by assuming $\alpha = \pi$, $\gamma = \frac{1}{2}\pi$. For $\alpha+\gamma < \frac{1}{2}\pi$ the cylindrical menisci are concave and stable: no bifurcation with the family of modified unduloids arises.

1. Introduction

The behaviour of liquid menisci at very low Bond numbers is receiving increasing attention owing to the possibilities of living and performing scientific research in the microgravity environment of space. The design of spacecraft tanks must ensure fuel outflow on demand. With the fuel no longer resting on the bottom and pistons not safely preventing bubble intrusion after several months in orbit, so-called surface-tension tanks are the obvious alternative. The surface energy of a liquid generally decreases when the liquid moves to concave regions of a container, i.e. in particular to corners and edges. Various surface-tension tanks based on longitudinal sections of circular cylinders and on rhombic cylinders have been tested, exploiting the short-time microgravity environment provided by parabolic flights of a KC-135 aircraft (Bauer 1986*a*; Langbein & Hornung 1989). Other designs foreseen for longer duration fights are being developed (Soo 1984).

During materials processing under microgravity conditions, the wetting of the crucible by the liquids or melts used is of primary importance as well. Changes in the contact angle may bring about significant changes in the liquid configuration. There have been several attempts to produce finely dispersed mixtures of monotectic alloys under microgravity conditions. When a melt of such an alloy is cooled down into the miscibility gap, separation of the melts is likely to start in crucible corners and edges.

First, cooling generally has easy access to the corners and edges. Secondly, the free energy of nucleation of a melt exhibiting a small contact angle is generally diminished in corners and edges. This applies in particular if, close to the critical point (consolutal point), there is complete wetting (Cahn 1977, 1979), i.e. if one of the consolutal melts wets the crucible so much better than the other melt that Young's condition between the interfacial tensions and the contact angle has no solution and the former melt spreads along the crucible anyway. However, with ongoing cooling and separation the contact angle and hence the liquid configuration may radically change.

It was proven by Lord Rayleigh in the last century (1879, 1945) that a free liquid jet breaks if its length L exceeds its circumference $2\pi R$. This stability criterion also applies to a cylindrical liquid column supported by coaxial circular disks. When lengthened to $L \geqslant 2\pi R$, one half of the column widens, whereas the other half shrinks accordingly. This instability is known as amphora-mode instability. It has been verified by using density matched liquids (Plateau simulation) and also by applying microgravity conditions. When the liquid column is rotating with circular frequency ω, the maximum stable length is reduced to $L = 2\pi R(1+\rho\omega^2R^3/\sigma)^{-0.5}$, where ρ is the density and σ the surface tension of the liquid considered. During the Skylab mission another instability of rotating liquid columns has been observed: the column may rotate around the axis like a skipping rope (Carruthers *et al.* 1975). This skipping-rope instability arises if $L \geqslant \pi R(\rho\omega^2R^3/\sigma)^{-0.5}$. During the Spacelab-D1 mission, the bifurcation in the breaking of rotating columns following the amphora-mode and the skipping-rope instabilities has been studied (Martinez 1987). In the five breakages performed, each time the amphora-mode instability won the race against the skipping-rope instability. The stability limits considered also hold for two liquids columns, each of one-half of the relevant length, if they are connected by a tube providing pressure and volume balance (Boys 1959).

The stability limits of liquid configurations may be conveniently calculated from the minimum volume condition. If a family of solutions of the capillary equation (or Gauss–Laplace equation) comprises two neighbouring solutions with equal liquid volume, but differing pressure, the liquid surface may be deformed without requiring energy, i.e. an unstable situation has been reached. In order to elucidate this principle, note that the capillary equation is the Lagrange equation resulting from minimizing the liquid energy under the constraint of constant liquid volume. The pressure is the respective Lagrange multiplier. This formalism, however, makes use of an extremum of the energy only: a solution of the capillary equation found may represent a saddle point rather than a minimum of the liquid energy. One has to make sure that there is not any infinitesimal deformation of the liquid surface leading to an even lower energy. This may be achieved by transforming the quadratic form of the liquid energy to main axes. If any of the respective eigenvalues is zero or even negative, an unstable surface has been found. A zero eigenvalue arises if two neighbouring solutions of the capillary equation exhibiting equal liquid volume are found. In that case there is no longer a force restoring the initial surface shape. The third variation of the liquid energy with respect to the surface deformation determines to which side the liquid surface is going to move. This gives rise to the minimum volume condition, which correctly should be called the extremum volume condition.

Numerous analytical and numerical stability diagrams valid for liquid columns between coaxial circular disks have been reported in terms of Bond number, circular frequency of rotation and ratio of the disk diameters (Heywang 1956; Corriell, Hardy

& Cordes 1977; Martinez 1983; Meseguer 1983; Langbein & Rischbieter 1984; Martinez, Haynes & Langbein 1987). Experimental observation of these stability limits has proven a sensitive method for measuring Bond numbers and surface tensions (Padday 1983; Langbein 1987). These investigations have been strongly stimulated by the fact that liquid columns represent a convenient geometry for measurements and calculations of resonance frequencies and Marangoni convection (Bauer 1984, 1986*b*; Schwabe & Scharmann 1979; Preisser, Schwabe & Scharmann 1983), and by the applicability of the results to the molten zones created during crystal growth with a free fluid surface according to the Czochralski or the travelling heater method.

2. Wetting of edges

Up to now little attention has been given to the stability of liquid volumes attached to solid edges. By a solid edge we mean wedges (with dihedral angle $2\alpha < \pi$) and edges in their more common sense (with dihedral angle $2\alpha > \pi$), see figure 1. The edge with dihedral angle $2\alpha = \pi$ is just a straight line on a plane.

At such edges a family of cylindrical surfaces exists. It has been shown by Concus and Finn that these cylindrical surfaces represent the state with minimum energy, if the sum of half the dihedral angle α and the contact angle γ is smaller than a right angle (Concus & Finn 1974; Finn 1986),

$$\alpha+\gamma < \tfrac{1}{2}\pi. \tag{1}$$

Equation (1) implies that the meniscus is concave, such that a capillary underpressure favouring penetration of the liquid into the wedge arises. On the ground and even more so under reduced gravity (at low Bond numbers), the liquid meniscus in such a wedge assumes a hyperbolic profile.

On the other hand, it is hard to believe that the cylindrical surface shown in figure 2 might be stable. Experience tells us that it will break into drops. Whenever the sum of half the dihedral angle α and the contact angle γ exceeds a right angle,

$$\alpha+\gamma > \tfrac{1}{2}\pi, \tag{2}$$

a convex meniscus causing capillary overpressure arises. A liquid column produced at such an edge may loose energy by breaking into droplets, if the edge is sufficiently long. Stability criteria similar to those valid for free columns may be expected. In the following we calculate the dependence of these stability limits on the dihedral angle 2α, the contact angle γ and the liquid volume. The calculations include free liquid columns via the dihedral angle $2\alpha = 2\pi$ and the contact angle $\gamma = \frac{1}{2}\pi$.

Breakage of the cylindrical surfaces shown in figures 1 and 2 will start, if there is an infinitesimal periodic deformation of the surface, which does not require energy. The stability limit $L = 2\pi R$ of the free cylindrical surfaces is conveniently obtained by embedding them into the family of unduloids. The cylinders in this context are unduloids with equal minimum and maximum radii. The bifurcation of both families of solutions gives the stability criterion.

In the following we proceed in similar manner. As a first step, we identify a family of azimuthally modified unduloids. The family of regular unduloids does not contain solutions which would fit to a solid edge with constant contact angle γ along the contact line (except if the contact angle equals $\frac{1}{2}\pi$). This requirement, rather, brings about non-axisymmetric deformations of the liquid surface. Therefore, in §§3 and 4 we construct a family of such non-axisymmetric solutions of the capillary equation.

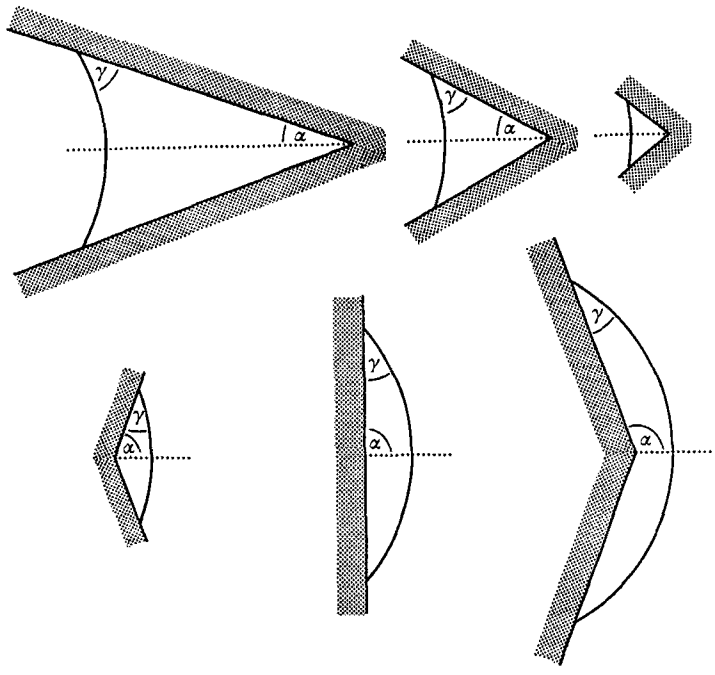

FIGURE 1. Concave and convex liquid menisci for $\alpha+\gamma \lesseqgtr \frac{1}{2}\pi$, corresponding to negative and positive fluidstatic pressure, at a solid edge.

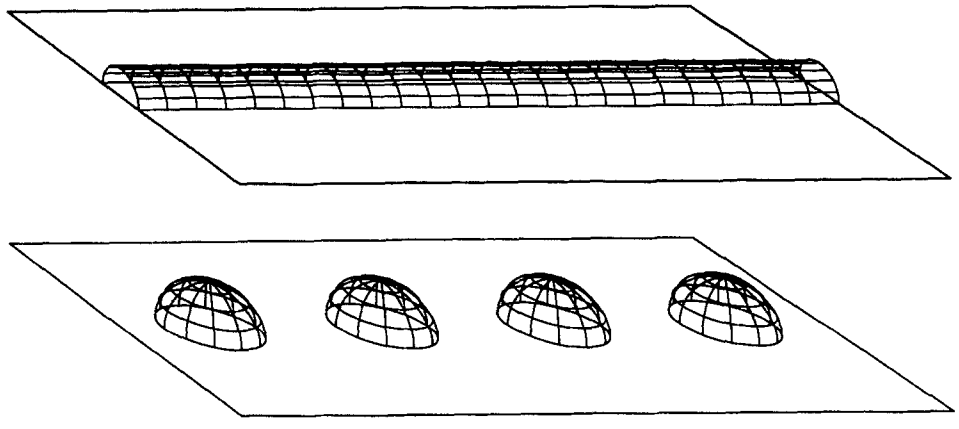

FIGURE 2. The breakup of a cylindrical column with contact angle $\gamma = \frac{1}{2}\pi$ on a plane (in an edge with dihedral angle $2\alpha = \pi$).

We consider small deviations d from the cylindrical shape and expand the liquid surface into a Fourier series with wavenumber q in the axial direction. We find the coefficients of this expansion to become Fourier series with wavenumber s in the azimuthal direction, such that a double Fourier expansion in the axial and azimuthal directions arises. The wavenumber s in the azimuthal direction may become imaginary, in which case a representation by hyperbolic cosines rather than by circular cosines results. The liquid surfaces obtained start off at zero azimuth like unduloids, but exhibit an azimuthal deformation increasing from $\varphi = 0$ to $\varphi = \pm\pi$,

where they intersect themselves. They therefore may come into existence only if they contact a third medium.

The position of the z-axis of the azimuthally deformed surfaces under construction need not be fixed before their adaptation to a solid edge. This is done in §5 by requiring that it coincides with the axis of the cylindrical solutions exhibiting the same liquid volume per length. Any other choice of the axis would considerably impede the calculation of the bifurcation of the surfaces considered with the cylindrical surfaces. Subsequently, the equation for the contact line with the solid edge is derived and constancy of the contact angle is required. This condition relates the wavenumber of the surfaces considered to the contact angle γ and the dihedral angle 2α of the edge.

The liquid volume per length is calculated in §6. It turns out not to depend on the azimuthal deformation to first order of the waveness parameter d, if the liquid column considered has infinite length or extends over an integer number of wavelengths $L = 2\pi/q$. In these cases the minimum volume condition is fulfilled: the shape of the liquid surface may be deformed without the need for external energy, i.e. a stability limit is reached. Among these stability limits, that corresponding to a single wavelength is the really important one. If the column is longer, it is unstable anyway. The respective stability criteria are discussed in detail in §7.

3. Axially periodic meniscus shapes

Using cylinder coordinates r, φ, z, the surface area of a liquid meniscus is

$$A = \int \mathrm{d}z \int r \,\mathrm{d}\varphi \left[1 + \left(\frac{\partial r}{r\,\partial\varphi}\right)^2 + \left(\frac{\partial r}{\partial z}\right)^2\right]^{\frac{1}{2}}, \tag{3}$$

and the liquid volume equals

$$V = \int \mathrm{d}z \int r \,\mathrm{d}\varphi \,\tfrac{1}{2} r. \tag{4}$$

Minimizing the surface energy σA of the liquid under the constraint of constant liquid volume V yields the Gauss–Laplace equation (capillary equation)

$$\frac{p}{\sigma} = \frac{1}{r\left[1 + \left(\frac{\partial r}{r\,\partial\varphi}\right)^2 + \left(\frac{\partial r}{\partial z}\right)^2\right]^{\frac{1}{2}}} - \frac{\frac{\partial}{r\,\partial\varphi}\left(\frac{\partial r}{r\,\partial\varphi}\right)\left[1 + \left(\frac{\partial r}{\partial z}\right)^2\right] - \frac{\partial r}{r\,\partial\varphi}\frac{\partial r}{\partial z}\left[\frac{\partial}{r\,\partial\varphi}\frac{\partial r}{\partial z} + \frac{\partial}{\partial z}\frac{\partial r}{r\,\partial\varphi}\right] + \frac{\partial^2 r}{\partial z^2}\left[1 + \left(\frac{\partial r}{r\,\partial\varphi}\right)^2\right]}{\left[1 + \left(\frac{\partial r}{r\,\partial\varphi}\right)^2 + \left(\frac{\partial r}{\partial z}\right)^2\right]^{\frac{3}{2}}}, \tag{5}$$

where σ is the surface tension, p the fluidstatic pressure difference across the liquid surface. Being interested in small deviations from the cylindrical shape, we restrict ourselves up to §8 to terms bilinear in $\partial r/r\,\partial\varphi$, $\partial r/\partial z$, etc. Equation (5) thus reduces to

$$\frac{p}{\sigma} = \frac{1}{r}\left[1 + \frac{1}{2}\left(\frac{\partial r}{r\,\partial\varphi}\right)^2 - \frac{1}{2}\left(\frac{\partial r}{\partial z}\right)^2\right] - \frac{\partial^2 r}{(r\,\partial\varphi)^2} - \frac{\partial^2 r}{\partial z^2}. \tag{6}$$

The breakage of infinite liquid columns, whether free or attached to a solid edge, is

axially periodic. The deformation therefore can be expanded into a Fourier series with axial wavenumber q:

$$r(\varphi, z) = \sum_{k=-\infty}^{+\infty} r_k(\varphi) \exp(\mathrm{i}kqz). \tag{7}$$

Owing to the structure of (5) and (6), $r_k(\varphi)$ is found to exhibit the order k in the deviation from the cylindrical shape. In zero order, $k = 0$, we obtain

$$r_0(\varphi) = \sigma/p = 1. \tag{8}$$

Equating the length σ/p to 1 means normalizing all other lengths to σ/p, too.

The first-order terms $k = \pm 1$ in (7) yield

$$-\frac{\mathrm{d}^2 r_{\pm 1}(\varphi)}{\mathrm{d}\varphi^2} = [1-q^2] r_{\pm 1}(\varphi). \tag{9}$$

Equation (9) is solved as

$$r_{\pm 1}(\varphi) = d_{\pm 1} \cos(s\varphi), \tag{10}$$

where

$$q^2 + s^2 = 1. \tag{11}$$

In (10) the sine term has been omitted, since we are interested in even functions of φ only. Odd functions do not fit the edges considered. In order for the deviation from the cylindrical shape to be real and small we require

$$d_{+1} = d_{-1} \equiv d \ll 1. \tag{12}$$

4. Second-order contributions

By substituting (8) and (10) into (6) and Fourier decomposition with respect to z, we obtain for the terms of order $k = \pm 2$ in the deviation from the cylindrical shape

$$-\frac{\partial^2}{\partial\varphi^2}[r_0(\varphi)-1] = [r_0(\varphi)-1] + \tfrac{1}{2}d^2[(3-4q^2)\cos(2s\varphi) + (1-2q^2)] \tag{13}$$

and

$$-\frac{\partial^2 r_{\pm 2}(\varphi)}{\partial\varphi^2} = (1-4q^2) r_{\pm 2}(\varphi) + \tfrac{1}{4}d^2[3(1-2q^2)\cos(2s\varphi) + (1-4q^2)]. \tag{14}$$

The terms $\cos(2s\varphi)$ in the aximuthal direction arise from products of first-order terms. The inhomogeneous solutions of (13) and (14) are given by

$$r_0(\varphi) - 1 = \tfrac{1}{2}d^2[\cos(2s\varphi) + (1-2s^2)], \tag{15}$$

$$r_{\pm 2}(\varphi) = -\tfrac{1}{4}d^2[(1-2s^2)\cos(2s\varphi) + 1]. \tag{16}$$

The homogeneous solutions of (13) and (14) are not further considered here, since they represent (i) a displacement of the column normal to its axis, which is fixed only in the next Section; (ii) an axial deformation of the column with wavenumber $2q$ which, if this is the leading deformation, is included in the present investigations by replacing $2q$ by q.

Gathering up (7), (8), (10), (15) and (16) we obtain

$$\begin{aligned} r(\varphi, z) = {} & 1 + 2d\cos(s\varphi)\cos(qz) \\ & + \tfrac{1}{2}d^2\{-\cos(2qz)[(1-2s^2)\cos(2s\varphi) + 1] + [\cos(2s\varphi) + (1-2s^2)]\}. \end{aligned} \tag{17}$$

By repeated substitution of the lower-order terms into (5) and evaluation of all products and square roots one obtains for $r(\varphi, z)$ the double Fourier series

$$r(\varphi, z) = \sum_{k=0}^{\infty} \sum_{l=0}^{\frac{1}{2}k} \sum_{m=0}^{\frac{1}{2}k} C(k, l, m)\, d^k \cos[(k-2l)\, s\varphi] \cos[(k-2m)\, qz]. \tag{18}$$

This series will be further discussed in §9.

5. Liquid menisci at solid edges

In order for a liquid meniscus to fit to a solid edge, the contact angle γ must be constant along the contact line. Let the distance of the z-axis from the planes forming the solid edge be h, see figure 3. Then, for the contact line we obtain the condition

$$r \sin(\varphi - \alpha) = h = \sin(\gamma - \tfrac{1}{2}\pi). \tag{19}$$

Substituting (17) into (19) and using

$$\varphi(z) = \alpha + \gamma - \tfrac{1}{2}\pi \tag{20}$$

at zero order, we find to first order of the waviness parameter d

$$\varphi(z) = \alpha + \gamma - \tfrac{1}{2}\pi - 2d \tan(\gamma - \tfrac{1}{2}\pi) \cos[s(\alpha + \gamma - \tfrac{1}{2}\pi)] \cos(qz). \tag{21}$$

The normal vector on the planes forming the solid edge equals

$$\boldsymbol{n}_s = (-\sin(\varphi - \alpha), -\cos(\varphi - \alpha), 0). \tag{22}$$

The normal vector on the liquid meniscus is given by

$$\boldsymbol{n}_l = \left(1, -\frac{\partial r}{r\,\partial \varphi}, -\frac{\partial r}{\partial z}\right) \Bigg/ \left[1 + \left(\frac{\partial r}{r\,\partial \varphi}\right)^2 + \left(\frac{\partial r}{\partial z}\right)^2\right]^{\frac{1}{2}}. \tag{23}$$

Hence, for the cosine of the contact angle we obtain

$$\boldsymbol{n}_s \cdot \boldsymbol{n}_l = \cos\gamma = \frac{-\sin(\varphi - \alpha) + \cos(\varphi - \alpha) \dfrac{\partial r}{r\,\partial \varphi}}{\left[1 + \left(\dfrac{\partial r}{r\,\partial \varphi}\right)^2 + \left(\dfrac{\partial r}{\partial z}\right)^2\right]^{\frac{1}{2}}}. \tag{24}$$

Substituting (21) for the contact line we are left with

$$\tan(\gamma - \tfrac{1}{2}\pi) = s \tan[s(\alpha + \gamma - \tfrac{1}{2}\pi)] + O[d^2]. \tag{25}$$

A liquid meniscus with constant contact angle γ along the contact line exists if (25) is satisfied. The second-order contributions to the meniscus shape according to (17) do not contribute to this condition. The third-order contributions considered in §9 cause terms of order d^2. The azimuthal wavenumber s is limited by $s^2 \leqslant 1$. It becomes imaginary for large axial wavenumbers q, such that the tangent in (25) becomes the hyperbolic tangent.

The condition of constant contact angle is part of the minimization of the liquid energy. It expresses the static equilibrium of forces acting at the contact line, i.e. of the three surface tensions involved. Experience, on the other hand, tells us that the contact angle changes significantly when a contact line is moving. An advancing contact angle generally is much larger than a receding contact angle, since the process of wetting requires additional energy against the viscous friction.

The dependency of the contact angle on the motion of the contact line, however,

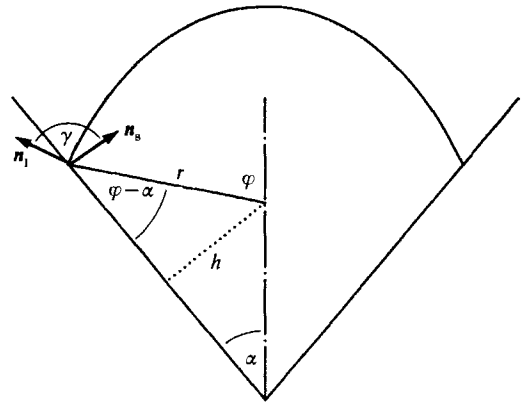

FIGURE 3. Sketch of the calculation of the contact line and the contact angle.

is irrelevant to the present investigations. The stability criteria used are static criteria. They result from minimizing the liquid energy. A variation of the contact angle during the process of breaking does not affect the stability limit.

It has been repeatedly quoted that it is also possible for the contact angle to show static hysteresis, i.e. that it may adopt different stable values along a stationary contact line. This non-moving of the contact line is explicitly excluded in the present investigations. It generally tends to extend the range of stability of liquid surfaces.

6. Constancy of the liquid volume

A stability limit arises if two neighbouring liquid surfaces enclosing the same liquid volume exist. From figure 3 we find

$$V = \int \mathrm{d}z \left\{ \int_0^{\varphi(z)} \mathrm{d}\varphi\, r^2 + h[r\cos(\varphi(z)-\alpha) + h\cot\alpha] \right\}. \tag{26}$$

$\varphi(z)$ is the azimuth along the contact line as given by (21). The integration over φ in (26) yields, inclusive of terms of second order $k = \pm 2$ in the waviness parameter d,

$$\begin{aligned} V = \int \mathrm{d}z \Big\{ & \Pi + 4d \frac{\sin[s(\alpha+\gamma-\tfrac{1}{2}\pi)]}{s} \cos(qz) \\ & + 2d^2(1-s^2)\left[(\alpha+\gamma-\tfrac{1}{2}\pi) + \frac{\sin[2s(\alpha+\gamma-\tfrac{1}{2}\pi)]}{2s}\right] \\ & + 4d^2[s\tan[s(\alpha+\gamma-\tfrac{1}{2}\pi)] - \tan(\gamma-\tfrac{1}{2}\pi)]\cos^2[s(\alpha+\gamma-\tfrac{1}{2}\pi)]\cos^2(qz) \Big\} \end{aligned} \tag{27}$$

where

$$\Pi = (\alpha+\gamma-\tfrac{1}{2}\pi) + \frac{\sin(\gamma-\tfrac{1}{2}\pi)}{\sin\alpha}\sin(\alpha+\gamma-\tfrac{1}{2}\pi) \tag{28}$$

is the cross-section of the cylindrical liquid volume fitting to the edge under consideration.

The terms of first order in the waviness d do not change the liquid volume if the

column has infinite length or extends over an integer number of wavelengths $L = 2\pi/q$. In that case we are left with

$$V = L\left\{\Pi + 2d^2(1-s^2)\left[(\alpha+\gamma-\tfrac{1}{2}\pi)+\frac{\sin[2s(\alpha+\gamma-\tfrac{1}{2}\pi)]}{2s}\right]\right.$$
$$\left.+\,2d^2[s\tan[s(\alpha+\gamma-\tfrac{1}{2}\pi)]-\tan(\gamma-\tfrac{1}{2}\pi)]\cos^2[s(\alpha+\gamma-\tfrac{1}{2}\pi)]\right\}. \quad (29)$$

For the liquid volume not to change also to second order of the waviness d, the main radius r_0 has to be adapted accordingly, e.g. (8) has to be replaced by

$$r_0 = 1-d^2\Pi^{-1}\left\{(1-s^2)\left[(\alpha+\gamma-\tfrac{1}{2}\pi)+\frac{\sin[2s(\alpha+\gamma-\tfrac{1}{2}\pi)]}{2s}\right]\right.$$
$$\left.+\,[s\tan[s(\alpha+\gamma-\tfrac{1}{2}\pi)]-\tan(\gamma-\tfrac{1}{2}\pi)]\cos^2[s(\alpha+\gamma-\tfrac{1}{2}\pi)]\right\}. \quad (30)$$

Taking into account (25) for constancy of the contact angle, we find the main radius r_0 generally to decrease and equivalently the pressure p to rise with increasing waviness d.

When the wetting case $\alpha+\gamma < \frac{1}{2}\pi$ is considered, r_0 and p apply to the exterior of the liquid attached to the edge. In that case we have from (30) that r_0 increases and p falls with increasing waviness d, which again means that the capillary pressure within the liquid attached to the edge rises.

7. The stability criterion

The family of liquid menisci, which fit to a solid edge with dihedral angle 2α, is defined by the double Fourier series (18), the dispersion relation (11) and the condition (25) on constancy of the contact angle. Equations (11) and (25) give two relationships between the waviness d, the axial wavenumber q and the azimuthal wavenumber s. One of these parameters can be chosen independently, i.e. a one-dimensional family of azimuthally modified unduloids fitting to the solid edge results. The structure of (11) and (25) suggests the use of the waviness d as the independent parameter.

The family of liquid menisci under consideration becomes unstable according to the minimum volume condition if two solutions resulting from each other by an infinitesimal deformation exhibit equal liquid volume. Since deformations involving a change in wavelength are by no means infinitesimal, the minimum volume condition is satisfied for zero waviness d at the bifurcation with the family of cylindrical menisci only. Equation (25) for $d = 0$ thus becomes the stability criterion.

When the liquid volume per length is normalized to the volume π of a free cylindrical column with radius 1,

$$\Pi = \pi, \quad (31)$$

figure 4 for the wavelength $L/2\pi = q^{-1}$ of breakage versus $\alpha+\gamma-\frac{1}{2}\pi$ results. The parameter for the different curves is α. The smallest stable length, $L/2\pi = 1$, is for the case of the free cylindrical column, into which a half-plane has been introduced up to the axis. This case is covered in the present investigations by assuming $\alpha = \pi$, $\gamma = \frac{1}{2}\pi$. It is indicated in figure 4 by a star.

From figure 4 it is obvious that there is a lower limit for the stable length depending on $\alpha+\gamma-\frac{1}{2}\pi$ only:

$$L/2\pi > [\pi/(\alpha+\gamma-\tfrac{1}{2}\pi)]^{\frac{1}{2}}. \quad (32)$$

This is further stressed in figure 5, where the squared wavenumber q^2 has been

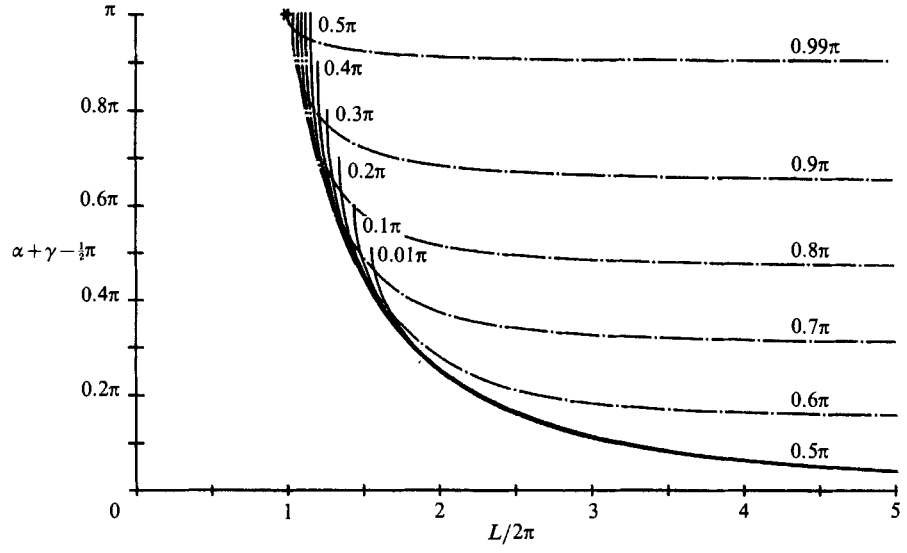

FIGURE 4. The wavelength $L/2\pi$ of breakage of liquid columns with cross-section $\Pi = \pi$ at a solid edge versus $\alpha+\gamma-\frac{1}{2}\pi$. The parameter for the different curves is half the dihedral angle α of the edge.

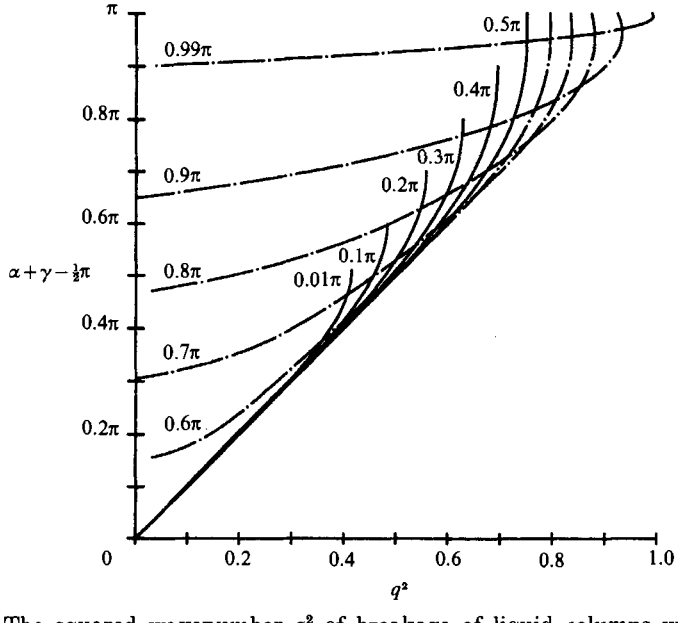

FIGURE 5. The squared wavenumber q^2 of breakage of liquid columns with normalized cross-section $\Pi = \pi$ at a solid edge versus $\alpha+\gamma-\frac{1}{2}\pi$. The parameter for the different curves is half the dihedral angle α of the edge.

plotted versus $\alpha+\gamma-\frac{1}{2}\pi$ (once again assuming the liquid volume per length to equal π).

For $\alpha+\gamma-\frac{1}{2}\pi < 0$, (25) has no solution, i.e. there is no bifurcation between the families of cylinders and modified unduloids. Concave cylindrical surfaces are always stable. This is the wetting situation described by (1).

8. The surface energy

The total surface of the liquid volume is made up by the free liquid surface A_1 and the contact area A_s with the solid edge. For the effective surface area

$$A_0 = A_1 - \cos\gamma A_s \tag{33}$$

we obtain

$$A_0 = 2\int dz\left\{\int_0^{\varphi(z)} d\varphi\left[r^2+\left(\frac{\partial r}{\partial\varphi}\right)^2+\left(r\frac{\partial r}{\partial z}\right)^2\right]^{\frac{1}{2}}+\sin(\gamma-\tfrac{1}{2}\pi)\,[r\cos(\varphi(z)-\alpha)+h\cot\alpha]\right\}. \tag{34}$$

Integration over φ in (34) yields

$$A_0 = 2\int dz\left\{\Pi+2d\frac{\sin[s(\alpha+\gamma-\frac{1}{2}\pi)]}{s}\cos(qz)\right.$$
$$\left.+2d^2(1-s^2)\left[(\alpha+\gamma-\tfrac{1}{2}\pi)+\frac{\sin[2s(\alpha+\gamma-\frac{1}{2}\pi)]}{2s}\right]\sin^2(qz)\right\}. \tag{35}$$

By integration over z over an integer number of wavelengths the first-order contribution to the effective surface area vanishes (as does the respective contribution to the liquid volume). In the second-order contribution $\sin^2 qz$ is replaced by $\frac{1}{2}$. We thus are left with

$$A_0 = 2L\left\{\Pi+d^2(1-s^2)\left[(\alpha+\gamma-\tfrac{1}{2}\pi)+\frac{\sin[2s(\alpha+\gamma-\frac{1}{2}\pi)]}{2s}\right]\right\}. \tag{36}$$

Substituting (30) for constancy of the liquid volume we eventually find

$$A_0 = 2L\{\Pi-d^2[s\tan[s(\alpha+\gamma-\tfrac{1}{2}\pi)]-\tan(\gamma-\tfrac{1}{2}\pi)]\cos^2[s(\alpha+\gamma-\tfrac{1}{2}\pi)]\}. \tag{37}$$

The effective surface area is not changed to second order of the waviness d, if condition (25) for the constancy of the contact angle along the contact line is satisfied. This confirms that (25) for $d = 0$ is the stability condition.

Going beyond this necessary condition, we may conclude from (37) that the total surface energy of the cylindrical surfaces is diminished by any deformation, the axial wavenumber of which exceeds that given by the stability criterion (25), even if the deformation does not satisfy the condition of constant contact angle. Deformations with wavelengths longer and shorter than that corresponding to (25) are stable and unstable, respectively.

9. Higher order contributions

For calculating the stability criterion from the minimum volume condition it is sufficient to consider terms up to order $k = 2$ in the waviness parameter d. To find the direction in which the respective deformation is going to become unstable, it is necessary to consider the terms of order $k = 3$. The terms of higher order are required to check convergence of the series expansion (18) and to enable reasonable first guesses for numerical calculations of surface shapes in more complicated configurations.

All terms up to order $k = 10$ in the deformation parameter d have been calculated by means of a computer program. It is based on subprograms, which from the coefficients $C(k,l,m)$ of threefold power and Fourier series like expression (18) calculate the coefficients $C(k,l,m)$ of products, quotients and square roots of such

threefold series. The calculation of the derivatives with respect to φ and z is straightforward anyway. By substitution of expression (18) into the capillary equation (5) and gathering up all terms of order $k = 3$, the computer program (and likewise a careful control by hand) yields

$$\begin{aligned} d^3\text{-terms in (17)} = &[(9q^2+9s^2-1)\,C(3,0,0)-(1-s^2)\,(1-7s^2)]\cos(3s\varphi)\cos(3qz) \\ &+[(q^2+9s^2-1)\,C(3,0,1)-(1-s^2)\,(1-3s^2)]\cos(3s\varphi)\cos(qz) \\ &+[(9q^2+s^2-1)\,C(3,1,0)-3(1-s^2)^2]\cos(s\varphi)\cos(3qz) \\ &+[(q^2+s^2-1)\,C(3,1,1)-3(1-s^2)^2]\cos(s\varphi)\cos(qz). \end{aligned} \tag{38}$$

Taking into account disperion relation (11) one obtains

$$C(3,0,0) = \tfrac{1}{8}(1-s^2)\,(1-7s^2), \tag{39}$$

$$C(3,0,1) = \frac{(1-s^2)\,(1-3s^2)}{8s^2}, \tag{40}$$

$$C(3,1,0) = \tfrac{3}{8}(1-s^2). \tag{41}$$

The fourth term in (38) is identical to the first-order contribution to $r(\varphi, z)$ according to (10) and (17). This term cannot be balanced by an appropriate choice of $C(3, 1, 1)$, but rather gives the d^2-contribution to the dispersion relation (11), which now reads

$$q^2+s^2 = 1+\tfrac{3}{2}d^2(1-s^2)^2+O(d^4). \tag{42}$$

The technique of the computer-aided successive satisfication of the capillary equation (5) is to balance by $C(k, l, m)$ all terms of order k in the waviness parameter d, which are caused by lower-order terms $n < k$ in the expansion of $r(\varphi, z)$. This balancing does not work for the first-order contribution $\cos(s\varphi)\cos(qz)$, since the respective coefficient $C(2k+1, k, k)$ contains the vanishing factor q^2+s^2-1. Each time the function $\cos(s\varphi)\cos(qz)$ is reobtained, i.e. at each odd order d^{2k+1} of the waviness parameter d, another contribution to the dispersion relation arises. The corresponding coefficients $C(2k+1, k, k)$ may be chosen arbitrarily, they just regenerate the first-order solution.

It turns out convenient to require

$$\sum_{l=0}^{\frac{1}{2}k}\sum_{m=0}^{\frac{1}{2}k} C(k,l,m) = 0. \tag{43}$$

Requiring (43) for $k > 1$, odd, means that this equation also holds for $k > 2$, even, i.e. that all higher-order contributions to the Fourier series (18) vanish for $s = 0$, $qz = 0, 2\pi$ and for $s = 0$, $qz = \pi$. Hence, $4d$ equals the maximum meniscus deformation along the symmetry plane $\varphi = 0$. From (43) we obtain

$$C(3,1,1) = -\frac{(1-s^2)\,(1+s^2-7s^4)}{8s^2}. \tag{44}$$

Substitution of the third-order contributions into (19) for the contact line and (25) for constancy of the contact angle yields the improved condition

$$\tan(\gamma-\tfrac{1}{2}\pi) = s\tan[s(\alpha+\gamma-\tfrac{1}{2}\pi)]+d^2\frac{(1-s^2)^3}{4s}\sin[2s(\alpha+\gamma-\tfrac{1}{2}\pi)]+O(d^4) \tag{45}$$

between the azimuthal wavenumber s and the waviness d. The contributions of the

terms $C(3,1,0)$ and $C(3,1,1)$ to (45) vanish identically, i.e. (45) is not affected by the choice of $C(3,1,1)$ according to (43).

Continuing with the solution of the capillary equation (5) to higher orders in the waviness parameter d one learns that the sensitive contributions are the terms $C(2k+1,l,k)\cos[(2k+1-2l)s\varphi]\cos(qz)$. During successive balancing of the inhomogeneous contributions, these terms regularly carry the factor $(2k-2l)(2k-2l+2)s^2$, compare (38). Hence, in the double Fourier series (18) another denominator s^2 arises at each odd order of k. The expansion with respect to the waviness d is actually an expansion with respect to d^2/s^2. For the Fourier series to converge

$$|d| \ll |s| \tag{46}$$

has to be required.

The coefficients $C(k,l,m)$ arising in the threefold series (18) actually may be represented by finite power series in s^2, i.e.

$$C(k,l,m) = \sum_{n=-\frac{1}{2}(k-1)}^{k-1} D(k,l,m,n)\,s^{2n}. \tag{47}$$

The higher-order contributions to the dispersion relation (11), (42) become power series in s^2 also,

$$q^2 = (1-s^2)\sum_{k=0}^{\infty}\sum_{n=-(k-1)}^{k-1} Q(k,n)\,[d^2(1-s^2)]^k s^{2n}. \tag{48}$$

The computer program described has been used for calculating the rational representation of all coefficients $D(k,l,m,n)$ in (47) up to order $k = 10$ and that of all coefficients $Q(k,n)$ in (48) up to order $k = 6$. They are filed in tables held in the *Journal of Fluid Mechanics* office and are obtainable from there on request. The numerical precision turned out not sufficient to obtain the rational form of the terms $k > 10$ as well. A further modification of the program based on the calculation of the coefficients $D(k,l,m,n)$ rather than on $C(k,l,m)$ would be necessary.

10. Conclusions

A liquid will spread along a solid edge under microgravity conditions if the sum of the contact angle γ and half the dihedral angle α is smaller than a right angle. In the opposite case, if the sum considered is larger than a right angle, a liquid volume initially pressed into the edge (e.g. by rotation) will be either sucked out or else will break, if the edge is sufficiently long. This principle can be efficiently used for measuring contact angles under microgravity conditions: take a series of wedges from the same solid material with differing dihedral angles 2α and observe which wedges are wetted by a given liquid and which are not. The precision of this method is limited by time only. When the limit $\alpha + = \frac{1}{2}\pi$ is approached from either side, wetting becomes very slow and the wavelength and time of breakage become very large.

This method can be applied not only to transparent liquids in transparent containers but also to metallic melts in high temperature crucibles. The wetting situation reached in a microgravity environment may be quenched and eventually inspected on ground. Recently, this method has been tested with transparent liquids during the short-time microgravity provided during the parabolic fight of an aircraft. An accuracy in the contact angle of water, glycerine and Fluorinert on glass and Plexiglas of a few degrees has been obtained (Langbein, Grossbach & Heide 1989).

Longer time microgravity experiments, to be performed in sounding rockets which provide about six minutes of microgravity are being planned.

A most interesting situation arises if a container is filled with two liquids with contact angles $\gamma_1 = \gamma, \gamma_2 = \pi - \gamma$, neither of which satisfies the wetting condition $\alpha + \gamma_i < \frac{1}{2}\pi$. In that case neither of the liquids may fully occupy the edge under consideration. If, owing to preceding changes in contact angle, one liquid wetted the edge or else was pressed into it by rotation, it will break into drops if the edge exceeds the relevant stability length. The resulting drops form spherical sections. Pronounced changes in contact angle happen in monotectic metallic melts, where close to the critical temperature complete wetting of the crucible by one melt has been predicted (Cahn 1977, 1979), whereas close to the monotectic temperature the above situation may arise. Another frequent reason for large changes in the contact angle is just contamination. If the change in contact angle considered is slow, it is likely that the liquid volumes, rather than breaking will be sucked into the container's corners.

The surface-tension tank suggested by the above considerations is a globe internally equipped with lamellae, the dihedral angles 2α between which narrow towards the poles. In regions where $\alpha + \gamma > \frac{1}{2}\pi$ the fuel will form drops between the lamellae, which lose capillary energy when moving towards the poles. A wetting fuel will reach regions where $\alpha + \gamma < \frac{1}{2}\pi$ and then be rapidly sucked to the poles. The drops of a non-wetting fluid slowly migrate between the lamellae towards the poles as well. However, they do not actually wet the edges themselves, but rather have to be sucked off the faces of the lamellae.

The reported theoretical investigations have been sponsored by the German Bundesminister für Forschung und Technologie (contract number QV 8723) in preparation of experimental tests on the behaviour of fluids in different containers during the short-time microgravity environment of parabolic flights.

REFERENCES

BAUER, H. F. 1984 Natural damped frequencies of an infinitely long column of immiscible viscous liquids. *Z. Angew. Math. Mech.* **64**, 475–490.

BAUER, H. F. 1986*a* Experiments on fluid interfaces in cylinders and cylindrical sections during parabolic flights of the KC-135 aircraft. *Forschungsber.* LRT-WE-9, University d. BW. München.

BAUER, H. F. 1986*b* Free surface and interface oscillations of an infinitely long liquid column. *Acta Astronautica* **13**, 9–22.

BOYS, C. V. 1959 *Soap bubbles: Their Colours and Forces which Mold Them*, pp. 58–62. Dover.

CAHN, J. W. 1977 Critical point wetting. *J. Chem. Phys.* **66**, 3667–3672.

CAHN, J. W. 1979 Monotectic composite growth. *Metall. Trans.* **10A**, 119–121,

CARRUTHERS, J. R., GIBSON, E. G., KLETT, M. G. & FACEMIRE, B. R. 1975 Studies of rotating liquid floating zones in Skylab IV. *AIAA-Paper* 75-692.

CONCUS, P. & FINN, R. 1974 On capillary free surfaces in the absence of gravity. *Acta Math.* **132**, 177–198.

CORIELL, S. R., HARDY, S. C. & CORDES, M. R. 1977 Stability of liquid zones. *J. Colloid Interface Sci.* **60**, 126–136.

FINN, R. 1986 *Equilibrium Capillary Surfaces.* Grundlehren der Mathematischen Wissenschaften. Vol. 284, pp. 1–244. Springer.

HEYWANG, W. 1956 Zur Stabilität senkrechter Schmelzzonen. *Z. Naturforschung* **11a**, 238–243.

LANGBEIN, D. 1987 The sensitivity of liquid columns to residual accelerations. *ESA*-SP 256, pp. 221–228.

LANGBEIN, D., GROSSBACH, R. & HEIDE, W. 1989 Parabolic flight experiments on fluid surfaces and wetting. *Appl. Microgravity Techn.* II, issue 4.

LANGBEIN, D. & HORNUNG, U. 1989 Liquid menisci in polyhedral containers. *Proc. Workshop on Differential Geometry, Calculus of Variations and Computer Graphics.* MSRI Book Series. Springer.

LANGBEIN, D. & RISCHBIETER, F. 1984 Form, Schwingungen und Stabilität von Flüssigkeitsgrenzflächen. *Schlussbericht für das BMFT*, 01 QV 242, pp. 1–130. Battelle Frankfurt/M. *Forschungsber.* W 86-029 *des BMFT.*

MARTINEZ, I. 1983 Stability of axisymmetric liquid bridges. *ESA*-SP 191, pp. 267–273.

MARTINEZ, I. 1987 Stability of long liquid columns in Spacelab-D1. *ESA*-SP 256, pp. 235–240.

MARTINEZ, I., HAYNES, J. M. & LANGBEIN, D. 1987 Fluid statics and capillarity. In *Fluid Science and Materials Science in Space* (ed. H. U. Walter), chap. II. Springer.

MESEGUER, J. 1983 The breaking of axisymmetric slender liquid bridges. *J. Fluid Mech.* **130**, 123–151.

PADDAY, J. F. 1983 *Fluid Physics in Space – The Kodak Ltd. Experiment aboard Spacelab-1.* Kodak Ltd.

PREISSER, F., SCHWABE, F. & SCHARMANN, A. 1983 Steady and oscillatory thermocapillary convection in liquid columns with free cylindrical surface. *J. Fluid Mech.* **126**, 545–567.

RAYLEIGH, LORD 1879 On the capillary phenomena of jets. *Proc. R. Soc. Lond.* **29**, 71–97.

RAYLEIGH, LORD 1945 *The Theory of Sound*, vol. 2, sect. 364. Dover (Reprint).

SCHWABE, D. & SCHARMANN, A. 1979 Some evidence for the existence and magnitude of a critical Marangoni-number for the onset of oscillatory flow in crystal growth melts. *J. Cryst. Growth* **46**, 124–131.

SOO, D. N. 1984 Study of slosh dynamics of fluid filled containers on 3-axis stabilized spacecraft. *Final Report of ERNO/ESTEC*, Contract 5238/83/NL/Bi(SC).